APPLICATIONS OF AlN THIN-FILM RESONATOR TOPOLOGIES AS ANTENNAS AND SENSORS

Robert J. Weber, Stanley G. Burns, Charles F. Campbell, Ron O'Toole
Department of Electrical Engineering and Computer Engineering
Iowa State University
Ames, Iowa 50011

ABSTRACT

The use of thin-film resonator (TFR) technology as on-wafer components is of considerable current interest. Cointegration of the TFR and active devices has been demonstrated. We report on two novel microwave applications of the TFR technology. The first application is the use of an array of TFRs as an on-wafer, phased-array antenna; the second is as a gas and chemical mass sensor with nanogram sensitivity.

INTRODUCTION

There is considerable recent interest in the development of thin-film bulk acoustic wave resonator technology for low-loss > 1GHz front-end filters for potential applications in communications systems, radar, and electronic-warfare systems [1]. In addition, sputter-deposited AlN thin-film resonators (TFR) have been used as the feedback frequency element in a variety of hybrid single-mode, comb-line, and voltage-controlled UHF and L-band oscillators [2-5]. Cointegration of the TFR and active devices has also been demonstrated where the piezoelectric material, AlN, was dc magnetron sputtered onto a p^+ doped silicon membrane whose function was to serve as an etch stop for the EDPW anisotropic etch used to remove substrate silicon [6-9]. We report on two additional novel applications of the TFR technology. The first application is the use of an array of TFRs as an on-wafer, phased-array antenna [10]; the second is as a gas and chemical mass sensor with nanogram sensitivity [11]. This paper will present an overview of the TFR technology with a focus on the implementation and experimental results of these two applications.

ANTENNA

Recently the thin-film resonator has been used as a feed and as a feed/radiator for microstrip antennas on semiconductor substrates. This technology, when fully developed, would allow for full wafer scale integration of microwave systems and provide a large amount of electromagnetic interference (EMI) protection. Note from Figure 1 that, using the feed as a simple stacked crystal filter, the ground plane provides an electrostatic shield between the front of the wafer and the back of the wafer. If this shield is completely enclosed by bonding the edges of the shield to a housing, the only path for energy to get from the front of the wafer to the back side of the wafer is acoustically.

The present work being conducted for the antenna structure is in increasing the Q of the resonators on the semiconductor surface. Several processes are under consideration. The Q is limited by the ohmic losses of the resonator for those configurations in which the fields don't penetrate the semiconductor material and is limited by both the ohmic losses of the resonator and the dielectric losses of the semiconductor whenever the fields penetrate the surface of the semiconductor. Figure 2 shows a resonator bridge structure which will increase the Q of the resonator by raising the impedance of the resonator in the same manner as using an air bridge line on a MMIC.

This antenna structure is being developed using the TFR to excite the antenna electrodes as well as having the TFR structure/resonator resonating acoustically and radiating electromagnetically simultaneously. Phased array structures using several antenna structures coupled in a controlled phase pattern on a single or multiple wafer installation have been proposed.

A calculated transmission plot of an overmoded structure passband using a transducer on both sides of a 400 μm thick silicon wafer is shown in Figure 3. This plot assumes the appropriate acoustical matching can be accomplished. A single resonator response on an overmoded structure is shown in Figure 4. The circuit used to calculate these responses is shown in Figure 5. The circuit responses were calculated using EEsof's Touchstone™ program.

MASS SENSOR

Sauerbrey [12] demonstrated that bulk-acoustic wave resonators could be used as mass sensors. Analytically, the fundamental-mode resonant frequency shift is given by

$$\begin{aligned}\Delta f_s / f_s &= -(\rho D) / (\rho_s D_s) \\ &= -(2 f_s \rho D) / (\rho_s C_s)^{1/2} \\ &= -(2 f_s \Delta M) / (\rho_s C_s)^{1/2}\end{aligned} \qquad (1)$$

where ρ is the density of the deposited layer, ρ_s is the density of the resonator material, D is the thickness of the deposited layer, D_s is the thickness of the resonator, f_s is the initial fundamental-mode resonant frequency, C_s is the stiffness constant, and ΔM is the change in surface mass/unit area. We observe that sensitivity is enhanced if f_s is high and D is small. These conditions are satisfied using an AlN TFR, with lateral Au electrode dimensions of 400 μm x 400 μm, designed to operate at a fundamental-mode of 1 GHz, mass-loaded with organic, selectively adsorbing, monolayer films. More specifically, a 5 μm c-axis vertical AlN piezoelectric membrane is produced by dc magnetron sputtering Al in a low-pressure N_2 environment. The top electrode is prepared by e-beam sequential deposition of 20 nm Ti and 200 nm Au. The backside electrodes are made by isotropically etching Si from beneath the AlN membrane and sequentially using e-beam deposition of Ti and Au. Electrode dimensions are designed to match Z_o = 50 Ω with S-parameters obtained by using co-linear probes on 100 μm centers. A Butterworth-VanDyke equivalent circuit is used to model the TFR with parameters determined by a Touchstone™ optimization routine.

For example, a test methanol gas phase sensor uses methyl methacrylate (PMMA photoresist). Figure 6 illustrates the series resonant-frequency shift as a function of a series of known volumetric concentrations. This figure also shows that there is very little, if any, hysteresis, and the output frequency shift is reasonably linear. These preliminary results correspond to minimum detectable masses below 2 ng/cm^2 which is better than found in quartz microbalances which typically operate at much lower f_s. Additional details on the chemistry of the monolayer thio-containing organic compounds are found in recent issues of "Analytical Chemistry".

Currently, work is focusing on optimization of the TFR fabrication and development of the adsorbing films. The TFR processing is designed to be compatible with an f_T > 2.5 GHz trench-isolated BJT technology [13] so that associated signal processing and conditioning electronics can be included on the same die. Work proceeds towards the concept illustrated in Figure 7 where the outputs from two identical cointegrated TFR-controlled oscillators (one sensor TFR passivated, the second identical sensor TFR exposed to the sensing environment) are mixed to obtain a low-frequency baseband output proportional to the gas phase measured. This approach should enhance sensitivity and repeatability by effectively minimizing temperature-induced drift and mechanical aging.

ACKNOWLEDGMENTS

This work is supported by the two U. S. Dept. of Commerce grants through the Center for Advanced Technology Development, and the Department of Electrical Engineering and Computer Engineering, Iowa State University. The graduate students were supported by U. S. Dept. of Education Fellowships. The experimental work has been conducted at the Iowa State University Microelectronics Research Center.

REFERENCES

[1] S. V. Krishnaswamy, J. Rosenbaum, S. Horwitz, C. Vale, and R. A. Moore, "Compact FBAR Filters Offer Low-Loss Performance", Microwaves and RF, Sept. 1991, pp. 127-136.

[2] S. G. Burns and P. H. Thompson, "Design, Analysis, and Performance of UHF Oscillators Using Thin-Film Resonator-Based Devices as the Feedback Element", Proceedings of the IEEE 32nd Midwest Symposium on Circuits and Systems, 1989, pp. 1005-1010.

[3. M. M. Driscoll, S. V. Krishnaswany, R. A. Moore, and J. R. Szedon, "UHF Film Resonator Evaluation and Resonator-Controlled Oscillator and Filter Design Using Computer-Aided Design Techniques," 1985 *IEEE MTT-S International Symposium*.

[4] S. G. Burns, G. R. Kline, and K. M. Lakin, "Design and Performance of Oscillators Using Semiconductor Delay Lines", Proceedings of the IEEE Ultrasonics Symposium, 1987, pp. 369-373.

[5] P. H. Thompson, S. G. Burns, G. R. Kline, and R.J. Weber, "Design and Performance of Voltage-Controlled Oscillators Using TFR Stacked Crystal Filters", Proceedings of the 43rd Annual IEEE Symposium on Frequency Control, 1990, pp. 58-62.

[6] W. A. Burkland, A. R. Landin, G. R. Kline, and R.S. Ketcham, "A Thin-Film Bulk-Acoustic Wave Resonator Controlled Oscillator on Silicon", IEEE Electron Device Letters, Vol. EDL-8 (11), pp. 531-533, November 1987.

[7] H. Satoh, H. Suzuki, C. Takahashi, C. Narahara, and Y. Ebata, " A 400 Mhz One-Chip Oscillator Using an Air-Gap Type Thin Film Resonator, Proceedings of the Ultrasonics Symposium, 1987, pp. 363-368.

[8] R. J. Weber, S. G. Burns, and S. D. Braymen, "A Semiconductor Process for Cointegration of BAW Thin-Film Piezoelectrics with Microwave BJTs", Proceeding of the 1990 Ultrasonics Symposium, 1990, pp. 525-528.

[9] S. G. Burns, R. J. Weber, and S. D. Braymen,"High Frequency Oscillators Using Cointegrated BAW Thin-Film Piezoelectrics With Microwave BJTs", Proceedings of the 45th Annual Symposium on Frequency Control, 1991, pp. 207-211.

[10] Robert J. Weber, "Acoustically Coupled Antenna," US Patent 5,034,753, July 23, 1991.

[11] R. O'Toole, S. G. Burns, H. R. Shanks, A. D'Silva, R. J. Weber, and M. D. Porter, "Microwave Frequency Oscillators Based on AlN: Toward Integrated Chemical Sensors", Optical and Piezoelectric Sensors Symposium, of the Electrochemical Society, October 1990.

[12] G. Sauerbrey, Z. Physik, 1959, 155, 206.

[13] R. J.Weber, S. G. Burns, and S. D. Braymen, "High Frequency Oscillator Comprising Cointegrated Thin Film Resonator and Active Device," U.S. Patent No. 5,075,641, December 24, 1991.

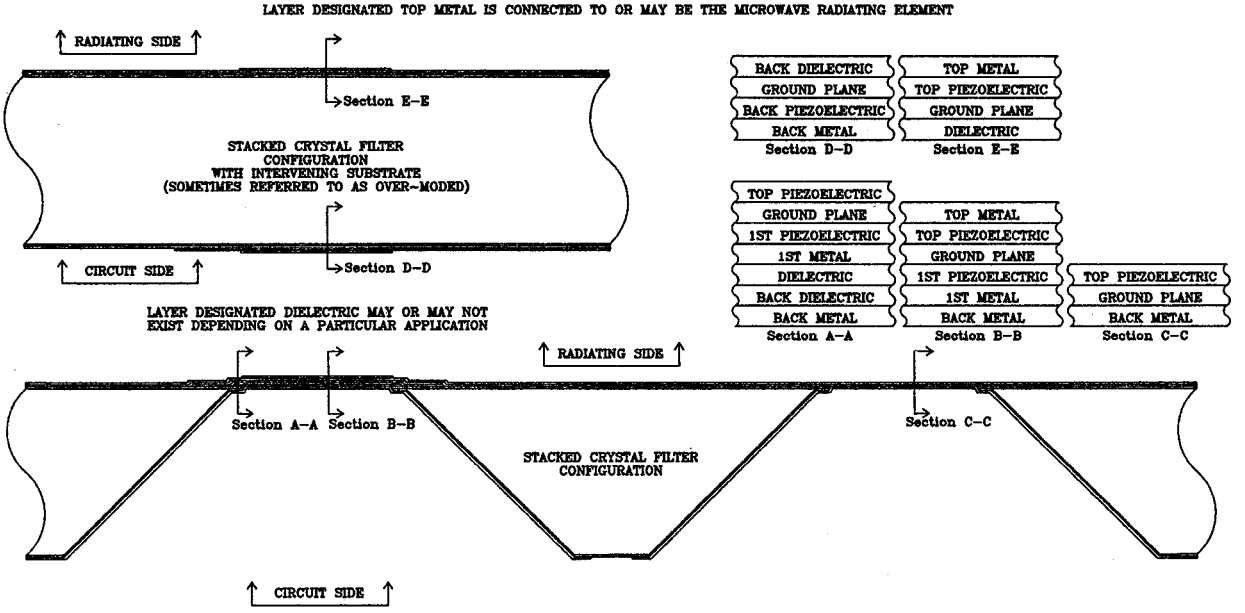

Figure 1. Antenna Resonator Transducer Cross Section.

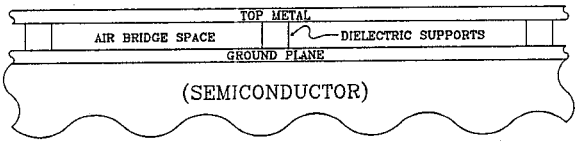

Figure 2. Air Bridge Resonator Cross Section.

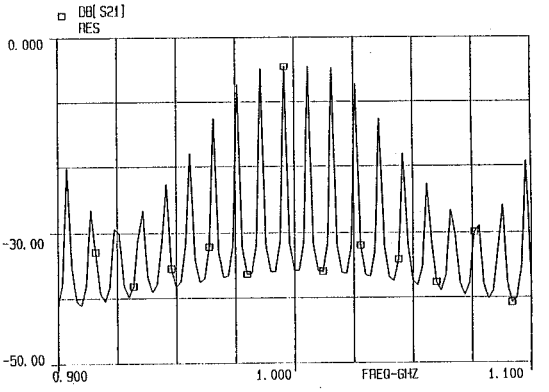

Figure 3. Calculated Transfer Function for an Overmoded Antenna Transducer Using a 400 μm Thick Silicon Substrate for a Given Set of Coupling Coefficients.

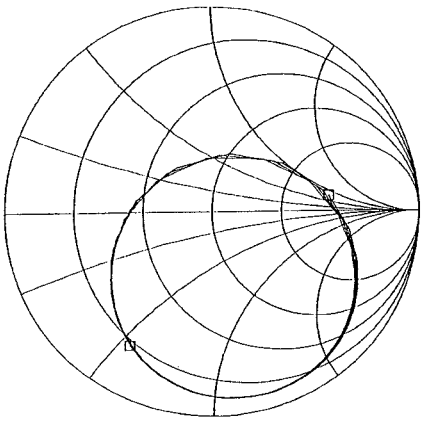

S_{11} Calculated

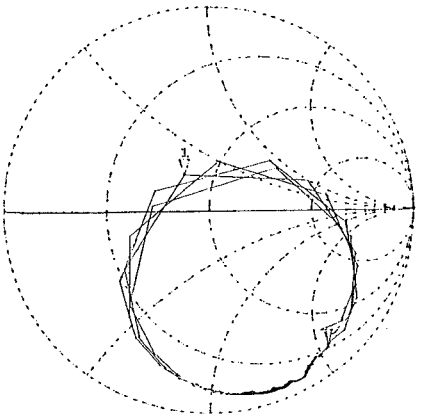

S_{11} Measured

Figure 4. Measured and Calculated Response for a Single Overmoded Resonator.

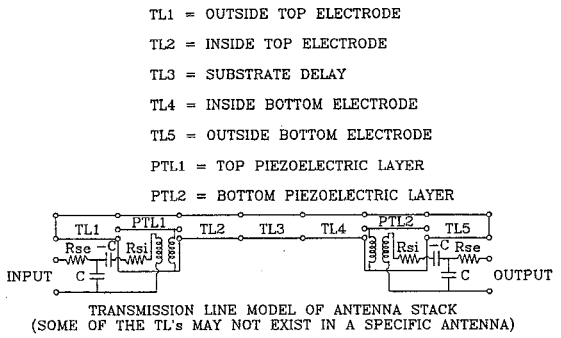

Figure 5. Equivalent Circuit Used to Calculate Responses.

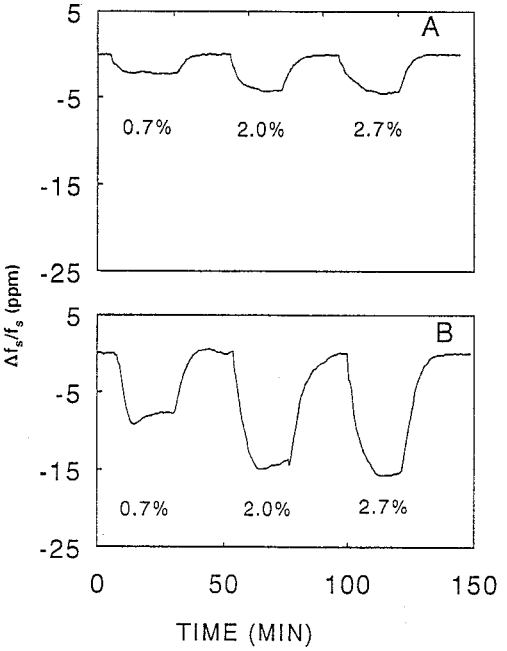

Figure 6. TFR f_s = 1GHz Responses With Hydrophobic and Hydrophilic Surfaces to Methanol. (A) TFR Coated With Fluorinated Thiolate. (B) TFR Coated With Carboxylic Acid-Terminated Thiolate. f_s Measurement Obtained From S_{21} Characteristics.

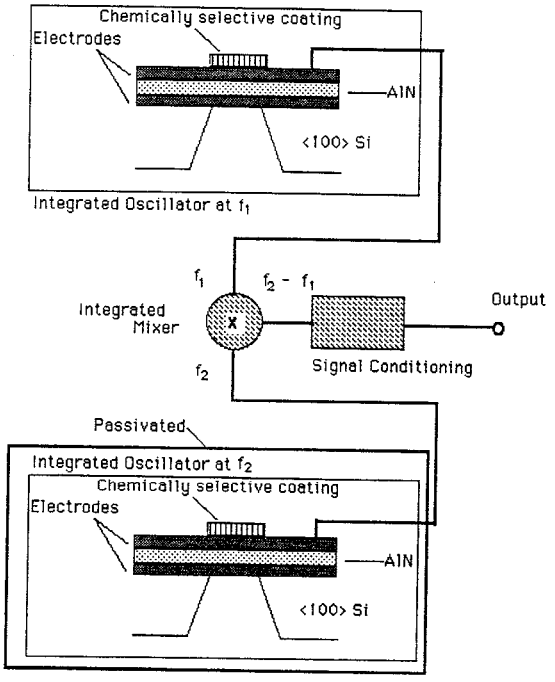

Figure 7. Proposed TFR Cointegrated Sensor Concept.